

## Collective core effects and dineutron correlations in three-body nuclei

J. CASAL<sup>(1)</sup>(\*), M. GÓMEZ-RAMOS<sup>(1)</sup> and A. M. MORO<sup>(1)</sup>(<sup>2</sup>)

<sup>(1)</sup> *Departamento de Física Atómica, Molecular y Nuclear, Facultad de Física, Universidad de Sevilla - Apartado 1065, E-41080 Sevilla, Spain*

<sup>(2)</sup> *Instituto Interuniversitario Carlos I de Física Teórica y Computacional (iC1) - Apdo. 1065, E-41080 Sevilla, Spain*

received 31 October 2023

**Summary.** — Two-neutron halo nuclei, such as  ${}^6\text{He}$ ,  ${}^{11}\text{Li}$  or  ${}^{14}\text{Be}$ , are known to have a marked (core +  $n + n$ ) three-body character, which is reflected in breakup, transfer or knockout reactions channels in nucleon-nucleon collisions. Their Borromean nature implies that the correlation between the valence halo neutrons is key to understand their properties, and their structure is also linked to spectra of the unbound core +  $n$  systems. Among other phenomena, the role of core collective excitations may be crucial to understand exotic properties such as parity inversion or shell gap quenching in the vicinity of nuclear halos and related systems. In this contribution it is shown that dineutron correlations can be successfully probed in proton-target knockout reactions, and that core excitation may be an important ingredient for a proper understanding of experimental observations.

### 1. – Introduction

Nuclei that present a three-body character have attracted particular interest over the past few decades. This is the case of two-neutron halo nuclei, understood as a compact core surrounded by two weakly bound neutrons, which exhibit exotic features in nuclear collisions [1]. A key feature of these systems is that they have a Borromean structure, *i.e.*, the core +  $n + n$  system is bound but the binary subsystems are unbound. Examples include  ${}^{11}\text{Li}$  or  ${}^6\text{He}$ , but also  ${}^{14}\text{Be}$ ,  ${}^{22}\text{C}$  or even  ${}^{29}\text{F}$  [2]. A good understanding of their properties and reaction dynamics requires knowledge of the low-lying spectrum of the unbound core +  $n$  subsystems, which can be populated in breakup, transfer or knockout reactions induced by two-neutron halos (*e.g.*, refs. [3-6]). But it is also clear that the correlation between the halo neutrons, often described in terms of pairing, is crucial to shape the halo physics [7, 8]. A spatially localized correlation of the halo neutrons is

(\*) E-mail: jcasal@us.es

usually referred to as dineutron configuration, a feature that is known to be favored if the system wave function contains large admixture of different-parity states [9]. It was proposed that the dineutron configuration may appear as a fundamental feature on the surface of neutron-rich nuclei [10, 11].

Since the seminal work by Tanihata *et al.* evidencing the halo character of  $^{11}\text{Li}$  in high-energy interaction cross section measurements [12], two-neutron halo nuclei have been extensively studied through various nuclear reactions. The spatial correlation associated to the dineutron have been studied in Coulomb dissociation and knockout reaction experiments [4, 13]. In this context,  $(p, pn)$  proton-target knockout reactions in inverse kinematics have been shown to provide very valuable spectroscopic information about the ground-state wave function and the spectrum of the unbound core +  $n$  residue [14, 15]. Recently, these reactions have been also employed to analyze dineutron correlations, by studying the correlation angle as a function of the intrinsic neutron momentum [16]. Various theoretical models have been employed to interpret those data.

A few-body description of neutron-halo nuclei and reactions involving them implies a clear distinction between the *core*, compact and often considered inert, and the *valence* neutrons. This separation may be reasonable for systems such as  $^6\text{He}$ , since the  $\alpha$  core requires about 20 MeV to get excited while the separation energy of the halo neutrons is of the order of 1 MeV [17, 18]. The inert core assumption, however, is not so well justified for more exotic systems. In [19, 20], core excitations were explicitly considered in the description of the one-neutron halo nucleus  $^{14}\text{Be}$ , showing important effects for low-energy reactions. Few-body calculations including core excitations have also been carried out for three-body nuclei, such as  $^{12}\text{Be}$  ( $^{10}\text{Be} + n + n$ ) and  $^{14}\text{Be}$  ( $^{12}\text{Be} + n + n$ ) [21, 22]. These models incorporate the excitation of the core by means of a collective particle-rotor picture with an effective deformation parameter. It is worth noting that core excitations have also been studied within the renormalized nuclear field theory [23, 24], where the coupling to quadrupole vibrations leads to parity inversion in  $^{11}\text{Be}$  and  $^{10,11}\text{Li}$ .

In this contribution, we focus on the neutron knockout from the Borromean halo nucleus  $^{14}\text{Be}$ , in connection to a recent systematic study including also  $^{11}\text{Li}$  and  $^{17}\text{B}$  [25]. We focus on the theoretical description of the  $(p, pn)$  process, outlining the basics of our few-body sudden reaction formalism and highlighting some key results.

## 2. – Formalism

In this work we describe the correlations in the  $(p, pn)$  process by using the eikonal sudden reaction formalism developed in refs. [26, 27] and employed in refs. [16, 25]. Within a three-body model for the Borromean projectile, it is shown that the transition amplitude can be written as

$$(1) \quad \mathcal{T} \propto \langle \phi_{2b}(\mathbf{k}_x, \mathbf{x}) \otimes e^{i\mathbf{k}_y \cdot \mathbf{y}} | S(y) \Phi_{3b}(\mathbf{x}, \mathbf{y}) \rangle,$$

where  $\Phi_{3b}(\mathbf{x}, \mathbf{y})$  is the initial ground-state wave function, described in Jacobi coordinates  $\{x, y\}$  (see fig. 1) with conjugate Jacobi momenta  $\{k_x, k_y\}$ , and  $\phi_{2b}(\mathbf{k}_x, \mathbf{x})$  represents a continuum state of the unbound core +  $n$  residue after one-neutron knockout from the halo. The above expression considers a zero-range  $V_{pn}$  interaction, and absorption effects are included through an eikonal  $S$ -matrix. More details about the relevant approximations are given in ref. [27]. Note that the bra-kets imply integration over the spatial coordinates.

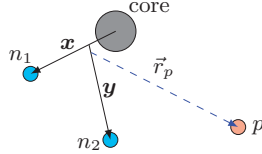


Fig. 1. – Scheme of the  $(p, pn)$  reaction and Jacobi coordinates.

The three-body ground-state  $\Phi_{3b}(\mathbf{x}, \mathbf{y})$  is obtained by solving the Schrödinger equation in hyperspherical coordinates [28]. For simplicity, this is done in the so-called Jacobi- $T$  representation, where the two valence neutrons are related by the  $x$  coordinate, and eigenstates are expanded in an analytical transformed harmonic oscillator basis [29]. Then, the wave function is rotated to the Jacobi- $Y$  coordinates shown in fig. 1, better suited to describe the knockout process. The continuum states  $\phi_{2b}(\mathbf{k}_x, \mathbf{x})$  describing the unbound core +  $n$  residual system are obtained by solving the two-body problem with scattering boundary conditions. The same core- $n$  interaction is employed to compute the two- and three-body states, ensuring a consistent description. Then, as discussed in ref. [27], the main structure ingredient is collected in the radial overlaps between  $\Phi_{3b}$  and  $\phi_{2b}$ . In particular, it is shown that Eq. (1) can be regarded as a distorted Fourier transform of the initial three-body ground state, the difference being introduced by the final state interactions in  $\phi_{2b}$  and the  $S$  matrix for the target proton. From the corresponding amplitudes, we get the cross sections as a function of the Jacobi momenta  $k_x, k_y$  and the correlation angle  $\theta$  between them (also called opening angle). Here,  $k_y$  corresponds to the momentum of the knocked-out neutron, typically referred to as intrinsic or missing momentum [16, 25].

### 3. – Results

We focus on the  $^{14}\text{Be}(p, pn)^{13}\text{Be}$  reaction at 265 MeV/nucleon, which was measured at RIBF-RIKEN [25]. Calculations were performed using the  $^{14}\text{Be}$  model already introduced in ref. [6] in the context of the transfer-to-the-continuum reaction framework [30]. This  $^{12}\text{Be} + n + n$  model is built on a  $^{13}\text{Be}$  unbound spectrum characterized most importantly by an  $s_{1/2}$  virtual state, a  $p_{1/2}$  resonance around 0.5 MeV above the neutron emission threshold, and a  $d_{5/2}$  resonance at around 2 MeV. The states are described with an effective core +  $n$  interaction with central and spin-orbit terms. As for the  $n$ - $n$  potential, we employ the effective interaction of ref. [31], which includes central and tensor terms. The coupling to the first  $2^+$  excited state of the  $^{12}\text{Be}$  core is included using a rotational scheme, with an effective deformation parameter  $\beta_2 = 0.8$ . As a consequence, the ground-state wave function of  $^{14}\text{Be}$  at 1.3 MeV below the three-body threshold contains  $\sim 20\%$  core-excited contributions. Looking at the partial-wave content,  $\sim 60\%$  of the total norm comes from  $p$ -wave components, which, mixed with the opposite parity  $s$ - and  $d$ -waves, leads to a marked asymmetry of the corresponding two-neutron density distribution [25].

From this structure input, we can compute intrinsic momentum and correlation angle distributions after knockout within our sudden reaction formalism. This requires an eikonal  $S$ -matrix for the  $p$ -core absorption. As detailed in ref. [27], we employ the  $t\rho$  prescription, generating Hartree-Fock densities with the SkX interaction [32] for the core. The modulus of the  $S$ -matrix is shown in fig. 2. It introduces absorption for small proton-core distances, which also corresponds to small core-neutron distances due to the

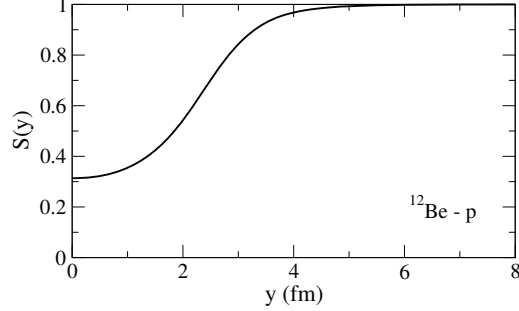


Fig. 2. – Modulus of the  $S$ -matrix for  $^{12}\text{Be}-p$  used in the calculation.

zero-range approximation for  $V_{pn}$ . Absorption is then more important at large intrinsic momenta exploring the nuclear interior.

In fig. 3 we show the opening angle distribution computed with the present model and compared with the experimental data, for an intrinsic momentum window up to  $k_y = 0.4 \text{ fm}^{-1}$ . In this region, the asymmetry of the angular distribution can be clearly seen, favoring large opening angles in momentum space. We can also compute the average correlation angle  $\theta$  as a function of the intrinsic neutron momentum  $k_y$ . Our results are shown in fig. 4 together with the experimental data. Both data and theory exhibit an average angle  $\langle \theta \rangle > 90^\circ$  in the region of small intrinsic momenta around  $0.2\text{-}0.3 \text{ fm}^{-1}$ . As discussed in refs. [16,25,27], this can be interpreted as a dineutron correlation probed precisely at the nuclear surface. It is worth noting that the asymmetry is coming from the mixing of the dominant  $p$ -wave content of the  $^{14}\text{Be}$  wave function with the opposite-parity  $s$ - and  $d$ -wave in the corresponding intrinsic-momentum region. The solid black line corresponds to the calculation in which the  $^{12}\text{Be}$  core in the final state after knockout can be in either its  $0^+$  ground state or its first  $2^+$  excited state, according to our structure model. We can see that this calculation tends to overestimate the data. Interestingly, looking at the contribution from the different core states reveals that the effect of the  $2^+$  excitation is an overall reduction of the average angle, diminishing the dineutron correlations. It is then foreseeable that a more sophisticated description of  $^{14}\text{Be}$ , including other excited states of the core, may improve the agreement between theory and data.

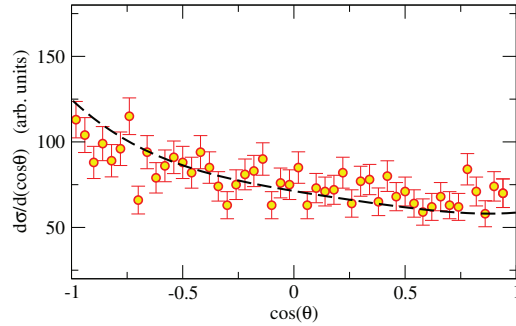


Fig. 3. – Correlation angle distribution gated for intrinsic momenta up to  $0.4 \text{ fm}^{-1}$  [25].

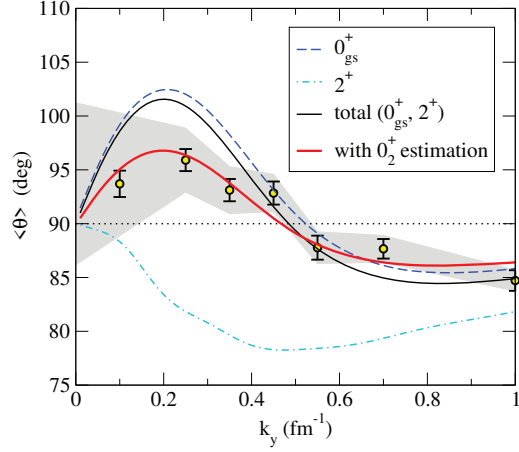


Fig. 4. – Average correlation angle as a function of the intrinsic momentum of the knocked-out neutron. Adapted from ref. [25]. The experimental uncertainties are given with statistical errors (bars) and an estimation of the systematic error (shaded area). The curves are the theoretical predictions, including core excitations.

The  $^{12}\text{Be}$  bound spectrum contains not only the  $0_{gs}^+$  ground state and  $2^+$  excited state considered above, but also a  $1^-$  state and a  $0_2^+$  isomer. The contribution from the latter may be significant, since it is likely to be populated in the reaction. Here we attempted an estimation of its effects, by considering that the  $0_2^+$  isomer is typically described as an orthogonal partner of the ground state [33]. This would imply opposite relative signs between its positive and negative-parity components. Taking this into account, the components with  $^{12}\text{Be}(0_2^+)$  should present  $\langle\theta\rangle < 90^\circ$  (opposite to those with  $^{12}\text{Be}(0_{gs}^+)$ ). By assigning to the  $^{12}\text{Be}(0_2^+)$  components a distribution equal to that of  $^{12}\text{Be}(0_{gs}^+)$  but mirrored around  $90^\circ$ , and a weight of 16% of the total wave function, this leads to the red solid line in fig. 4. We can see a better agreement with the data, though the estimation is only tentative. As already mentioned in ref. [34], core excitation may have a significant effect for the dineutron correlation. Theoretical developments in order to include all such components consistently are desirable.

\* \* \*

The authors are grateful to A. Corsi and Y. Kubota for useful discussions and for the experimental work and analysis behind the data shown here. This work has been partially funded by MCIN/AEI/10.13039/501100011033 under I+D+i project No. PID2020-114687GB-I00 and under grant IJC2020-043878-I (also funded by “European Union NextGenerationEU/PRTR”), by the European Union’s Horizon 2020 research and innovation programme under the Marie Skłodowska-Curie grant agreement No. 101023609, and by the Consejería de Economía, Conocimiento, Empresas y Universidad, Junta de Andalucía (Spain) and “ERDF-A Way of Making Europe” under PAIDI 2020 project No. P20\_01247.

## REFERENCES

- [1] TANIHATA I., SAVAJOLS H. and KANUNGO R., *Prog. Part. Nucl. Phys.*, **68** (2013) 215.
- [2] BAGCHI S. *et al.*, *Phys. Rev. Lett.*, **124** (2020) 222504.
- [3] AUMANN T. *et al.*, *Phys. Rev. C*, **59** (1999) 1252.

- [4] SIMON H. *et al.*, *Nucl. Phys. A*, **791** (2007) 267.
- [5] SANETULLAEV A. *et al.*, *Phys. Lett. B*, **755** (2016) 481.
- [6] CORSI A. *et al.*, *Phys. Lett. B*, **797** (2019) 134843.
- [7] ESBENSEN H., BERTSCH G. F. and HENCKEN K., *Phys. Rev. C*, **56** (1997) 3054.
- [8] HAGINO K. and SAGAWA H., *Phys. Rev. C*, **72** (2005) 044321.
- [9] CATARA F., INSOLIA A., MAGLIONE E. and VITTURI A., *Phys. Rev. C*, **29** (1984) 1091.
- [10] MATSUO M., *Phys. Rev. C*, **73** (2006) 044309.
- [11] HAGINO K., SAGAWA H., CARBONELL J. and SCHUCK P., *Phys. Rev. Lett.*, **99** (2007) 022506.
- [12] TANIHATA I. *et al.*, *Phys. Rev. Lett.*, **55** (1985) 2676.
- [13] NAKAMURA T. *et al.*, *Phys. Rev. Lett.*, **96** (2006) 252502.
- [14] KONDO Y. *et al.*, *Phys. Lett. B*, **690** (2010) 245.
- [15] AKSYUTINA Y. *et al.*, *Phys. Lett. B*, **718** (2013) 1309.
- [16] KUBOTA Y. *et al.*, *Phys. Rev. Lett.*, **125** (2020) 252501.
- [17] TILLEY D., WELLER H. and HALE G., *Nucl. Phys. A*, **541** (1992) 1.
- [18] TILLEY D. R. *et al.*, *Nucl. Phys. A*, **708** (2002) 3.
- [19] DE DIEGO R., ARIAS J. M., LAY J. A. and MORO A. M., *Phys. Rev. C*, **89** (2014) 064609.
- [20] PESUDO V. *et al.*, *Phys. Rev. Lett.*, **118** (2017) 152502.
- [21] NUNES F., THOMPSON I. and TOSTEVIN J., *Nucl. Phys. A*, **703** (2002) 593.
- [22] TARUTINA T., THOMPSON I. and TOSTEVIN J., *Nucl. Phys. A*, **733** (2004) 53.
- [23] BARRANCO F., POTEL G., BROGLIA R. A. and VIGEZZI E., *Phys. Rev. Lett.*, **119** (2017) 082501.
- [24] BARRANCO F., POTEL G., VIGEZZI E. and BROGLIA R. A., *Phys. Rev. C*, **101** (2020) 031305.
- [25] CORSI A. *et al.*, *Phys. Lett. B*, **840** (2023) 137875.
- [26] KIKUCHI Y., OGATA K., KUBOTA Y., SASANO M. and UESAKA T., *Prog. Theor. Exp. Phys.*, **2016** (2016) 103D03.
- [27] CASAL J. and GÓMEZ-RAMOS M., *Phys. Rev. C*, **104** (2021) 024618.
- [28] ZHUKOV M., DANILIN B., FEDOROV D., BANG J., THOMPSON I. and VAAGEN J., *Phys. Rep.*, **231** (1993) 151.
- [29] CASAL J., RODRÍGUEZ-GALLARDO M. and ARIAS J. M., *Phys. Rev. C*, **88** (2013) 014327.
- [30] MORO A. M., *Phys. Rev. C*, **92** (2015) 044605.
- [31] GOGNY D., PIRES P. and TOURREIL R. D., *Phys. Lett. B*, **32** (1970) 591.
- [32] ALEX BROWN B., *Phys. Rev. C*, **58** (1998) 220.
- [33] MACCHIAVELLI A. O. *et al.*, *Phys. Rev. C*, **97** (2018) 011302.
- [34] KOBAYASHI F. and KANADA-EN'YO Y., *Phys. Rev. C*, **93** (2016) 024310.